J. Membrane Biol. 163, 129–136 (1998)

The Journal of
Membrane
Biology

ATP-Induced Shape Change of Nuclear Pores Visualized with the Atomic Force Microscope

A. Rakowska, T. Danker, S.W. Schneider, H. Oberleithner
Department of Physiology, University of Münster, Robert-Koch-Str. 27a, D-48149 Münster, Germany

Received: 10 February 1997/Revised: 10 February 1998

Abstract. Bidirectional transport of molecules between nucleus and cytoplasm through the nuclear pore complexes (NPCs) spanning the nuclear envelope plays a fundamental role in cell function and metabolism. Nuclear import of macromolecules is a two-step process involving initial recognition of targeting signals, docking to the pore and energy-driven translocation. ATP depletion inhibits the translocation step. The mechanism of translocation itself and the conformational changes of the NPC components that occur during macromolecular transport, are still unclear. The present study investigates the effect of ATP on nuclear pore conformation in isolated nuclear envelopes from *Xenopus laevis* oocytes using the atomic force microscope. All experiments were conducted in a saline solution mimicking the cytosol using unfixed nuclear envelopes. ATP (1 mM) was added during the scanning procedure and the resultant conformational changes of the NPCs were directly monitored. Images of the same nuclear pores recorded before and during ATP exposure revealed dramatic conformational changes of NPCs subsequent to the addition of ATP. The height of the pores protruding from the cytoplasmic surface of the nuclear envelope visibly increased while the diameter of the pore opening decreased. The observed changes occurred within minutes and were transient. The slow-hydrolyzing ATP analogue, ATP-γ-S, in equimolar concentrations did not exert any effects. The ATP-induced shape change could represent a nuclear pore ''contraction.''

Key words: Nuclear pore complexes — ATP — Atomic force microscopy — Nuclear pore conformation

Correspondence to: H. Oberleithner

Introduction

The genetic material of a eukaryotic cell is enclosed by the nuclear envelope, a semipermeable barrier separating the nucleus from the cytoplasm. The passage of molecules between both cell compartments occurs through nuclear pore complexes (NPCs), supramolecular protein structures embedded in the nuclear envelope. A single NPC has a molecular mass of about 124 MD and has been described as a tripartite assembly consisting of a spoke complex, sandwiched between a cytoplasmic and a nuclear ring (for review, *see* [31]). Despite considerable progress towards a better understanding of the three-dimensional architecture of the NPC in recent years, the function of some specific pore components remains controversial. The NPC can appear plugged with a centrally located granule. This structure is thought to be an intrinsic protein structure of the NPC, the so-called central transporter, an important part of the molecular transport machinery [2, 8]. On the other hand, it cannot be ruled out that the granule is a mobile macromolecule on its transport route through the nuclear pore.

The NPCs accommodate both passive diffusion and active transport. The pioneering work of Loewenstein and Kanno published 35 years ago [18] presented the first electrophysiological evidence for a barrier function of the nuclear envelope. Recent electrophysiological data strongly indicate that the nuclear pores (or associated structures) determine the permeability of this barrier and thus can be envisioned as highly regulated transport channels. The electrical activity of those channels is thought to range from a virtually closed state (i.e., a few pS) to a wide open stage (i.e., more than 1000 pS) [6, 19, 20, 28]. Under certain conditions that are not fully understood, inorganic ions and small organic molecules can diffuse freely through a 10-nm aqueous channel within the NPC. The transport of large molecules, like proteins with a molecular weight larger than 40 kD and the RNA

transcripts, is an energy dependent and highly selective process [7, 27, 29]. In functioning as a ''gate-keeper'' for the nucleus, the NPC therefore offers means for the regulation of crucial cellular functions such as gene expression and subsequent protein synthesis.

The active import of macromolecules into the nucleus can be experimentally divided into two steps: signal-dependent docking to fibrils extending from the cytoplasmic ring of the pore, followed by an energy-driven translocation through the pore [25]. Both transport steps require distinct cytosolic and nuclear transport factors discovered over the last few years [21]. The initial signal recognition and docking to the cytoplasmic rim of the NPC is mediated by importin α and β, two proteins forming an essential cytosolic receptor complex. The importin complex interacts with the nuclear localization sequence of the import protein and docks the import substrate to the pore [13, 23]. The translocation step is ATP-dependent but part of the energy requirement seems to be also due to GTP hydrolysis by Ran, a small GTPase, and to the protein pp15 (=NTF2), which is another essential factor for the second phase of nuclear import (for review, *see* [12, 27]). ATP addition was reported to enhance and ATP depletion to inhibit active nuclear import of macromolecules [24, 33]. These findings are strongly supported by electrophysiological experiments showing that ATP increases the electrical conductance of the nuclear envelope [20]. The exact mechanisms underlying transport of inorganic ions and macromolecules through the nuclear pore remain unclear. Potential conformational changes of the nuclear pore involved in the translocation procedure have been addressed in several experiments [1, 8, 32] but need further elucidation.

The three-dimensional structure of the NPC has been extensively investigated by electron microscopy [1, 2, 10, 15, 30]. In the last few years, the atomic force microscope (AFM) has also become a useful tool for imaging the nuclear envelope and the surface of nuclear pores [8, 11, 28, 34]. The resolution achieved with the AFM in a complex biological preparation is usually lower than that obtained with the electron microscope. However, a decisive advantage of the AFM is its ability to scan unfixed material under physiological conditions (for review, *see* [16]). This new feature made it possible to examine conformational changes of native NPCs in response to ATP, the major substrate for nucleocytoplasmic transport. In the present study we show a shape change in the NPC structure induced by ATP in real time, imaged under physiological conditions.

Materials and Methods

Preparation of the Nuclear Envelope

Xenopus laevis were anesthetized in 0.1% ethyl m-aminobenzoate methane sulphonate (Serva, Heidelberg, Germany) and their ovaries were removed. Oocytes were dissected from ovary clusters and stored in Ringer solution (in mM): 87 NaCl, 3 KCl, 1 $MgCl_2$, 1.5 $CaCl_2$, 10 Hepes, 5.5 Glucose, pH 7.8) before use. After placing the oocytes in nuclear isolation medium (NIM; 90 KCl, 10 NaCl, 2 $MgCl_2$, 0.06 $CaCl_2$, 1.1 EGTA (buffers free Ca^{2+} to 10^{-8} M), 10 HEPES, pH 7.32) the nuclei were manually isolated by piercing the oocyte with two pincers. Individual intact nuclei were picked up with a pasteur pipette and transferred to a glass coverslip placed under a stereomicroscope. Then the chromatin was carefully removed using sharp needles and the nuclear envelope was spread on glass, with the nucleoplasmic side facing downwards. The specimen were washed with deionized water, dried shortly and rehydrated in NIM before the scanning procedure. The drying step was necessary to improve the adhesion of the nuclear envelope to the specimen support.

Use of the Atomic Force Microscope

For our experiments we used a BioScope™ (NanoScope III, Digital Instruments, Santa Barbara, CA) mounted on an inverted optical microscope (Axiovert 135, Zeiss, Jena, Germany). We used standard V-shaped 200 μm long silizium nitride cantilevers with spring constants of 0.06 N/m and pyramidal tips with an estimated tip diameter of 10 nm. The cantilevers were obtained from Digital Instruments. The images were recorded with 256 or 512 lines per screen, at constant force (height mode) with a scan rate of 1.5 Hz. The forces applied during the scanning procedure were minimized by, in a first step, retracting the AFM-tip until it lost contact with the sample surface and, in a second step, by reengaging the tip at a setpoint (i.e., force value) minimally above the liftoff value. Applying this approach, we usually could obtain scanning forces below 1 nN.

All scanning procedures were done in fluid (i.e., in NIM). After a control period of 15 min 100 μl of a 10 mM $MgATP_2$ (or 10 mM $MgATP_2$-γ-S if applicable) stock solution was added into 900 μl of NIM scanning fluid giving a final concentration of 1 mM ATP in the scanning solution. Thus, the use of magnesium salts prevented a change of free Mg^{2+} in NIM induced by the addition of ATP (or ATP-γ-S) that chelates Mg^{2+} at equimolar concentration. Images of a 16 μm^2 area of the preparation were usually recorded over a control period of at least 15 min followed by a period of up to 90 min after ATP addition.

The heights and diameter of individual NPCs before and after the addition of ATP were measured in cross-sections of the images using the Bioscope™ analysis software. The ''pore diameter'' measurement was taken from the highest, oppositely located points of the cytoplasmic ring in the cross section of the respective NPC. Since our experiments were performed in a paired fashion, the measured heights and diameters of individual NPCs after the addition of 1 mM ATP could be directly compared to their respective values before ATP addition (control).

Statistics

Results are given as mean values ± SEM. Significance of differences was evaluated applying the paired Student *t*-test if applicable. Significantly different is $P < 0.05$ or less.

Results

The advantages of high resolution combined with the ability to image unfixed preparations in fluid make the AFM a useful tool for investigating conformational

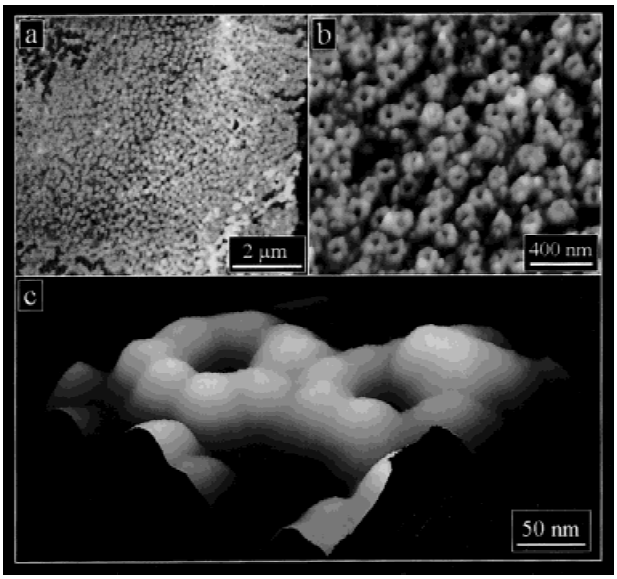

Fig. 1(*a–c*). AFM images showing the cytoplasmic face of native nuclear envelopes from *Xenopus laevis* oocyte nuclei scanned in air. (*a*) 64 μm^2 area showing the high density of nuclear pore complexes in the preparation. (*b*) 4 μm^2 area showing different nuclear pore configurations. Some pores appear plugged with central granules while the majority of pores appears unplugged. (*c*) Two enlarged nuclear pore complexes with visible subunits forming the cytoplasmic ring. (*b*) and (*c*) are zoomed images from (*a*).

changes of NPCs maintained in physiological conditions. Figure 1 shows AFM images of the cytoplasmic face of a native nuclear envelope from *Xenopus laevis* oocyte, scanned in air. The density of NPCs in a *Xenopus* oocyte nuclear envelope is about 40 nuclear pores per μm^2 (Fig. 1*a*). As evident from Fig. 1*b*, most NPCs are packed with particles, and some appear plugged (i.e., a central granule is visible). Distinct subunits of the cytoplasmic ring of the NPC are visible in Fig. 1*c*, revealing the eightfold symmetry of the nuclear pore complex. Plugged and unplugged nuclear pores are depicted in Fig. 2. Such NPC configurations can be found in one and the same preparation. The ''plug'' at the cytoplasmic face of the NPC is most likely a protein attached to the NPC surface.

In comparison to the dry preparation presented in Figs. 1 and 2, the lateral resolution of NPCs imaged in fluid is decreased (compare both Figs. 1 and 2 with Fig. 3). However, AFM-experiments under physiological conditions in fluid allow the direct monitoring of changes in NPC conformation (i.e., real time recordings) in response to various physiological stimuli.

Since NPC-mediated transport is known to be ATP-dependent we tested for any changes in the conformation of native NPCs after the addition of 1 mM ATP to the bath solution mimicking the electrolyte composition of the cytosol. Figure 3 shows a representative experiment. Over the entire period of the experiment a nuclear surface area of 16 μm^2 was imaged before (control) and during ATP application. Figure 3 shows four images (depicting the same area—4 μm^2— of the preparation) obtained over a time period of 90 min. The insets in this figure show the change in the profile of an individual NPC (marked with arrow) over time. The images show a transient shape change of the NPCs in response to ATP. The control image (Fig. 3*a*) was recorded 15 min after the start of the scanning procedure. Over this period of time the surface structures remained constant. During scanning (throughout the entire experiment) the scanning force was frequently tested and adjusted (if necessary) to the minimal value. The heights of the cytoplasmic rings of the NPCs in the control image range from 11 nm to 16 nm, measured from the base (nuclear envelope bilayer) to the top (NPC). The diameters of the NPCs vary between 70 nm and 117 nm. Pore openings (cytoplasmic mouths of the central channels) are visible in NPCs (*also see* profiles). The overall shape of the NPCs changes dramatically in response to ATP. During exposure to the nucleotide the NPCs grow in height and shrink in diameter. Figure 3*b* shows the same area of the nuclear envelope 2 min after the addition of 1 mM ATP. Pore measurements in this image reveal a mean increase in NPC height of 5.0 nm, while the diameter shrinks by 13.3 nm. The observed increase in NPC height is even more pronounced 10 minutes after the addition of ATP (Fig. 3*c*). NPCs increase in height by 8.1 nm while mean diameters decrease by 17.2 nm compared to the corresponding control values. The observed effect is clearly transient. After prolonged exposure to ATP nuclear pores relax and heights and widths of the NPCs again approach the respective control values 90 min after the start of the experiment, heights and diameters of NPCs are found not significantly different from their corresponding control values ($n = 10$, $P > 0.05$). Figure 4*a* and *b* show the individual heights above the nuclear envelope (measured from the lipid bilayer to the NPC top) and the diameters of 10 nuclear pores at different time intervals after the addition of ATP. The corresponding mean values (±SEM) are depicted in Fig. 4*c* and *d*.

Table 1 presents a summary of the ATP experiments on all nuclear envelopes examined. Obviously, not all preparations responded to (hydrolyzable) ATP. As presented in the lower part of Table 1 (nuclear envelopes VIII-X), in about 30% of the nuclear envelopes examined virtually no response was observed after the addition of ATP. A possible explanation could be an ''overstretching'' of the nuclear envelope during the preparation process, leading to significant leaks in the calcium stores of the cisternae. Calcium-filled stores, however, are known to be a prerequisite for normal nuclear pore function (for details, *see* Discussion).

To test whether ATP binding or ATP hydrolysis was responsible for the dramatic changes in pore conforma-

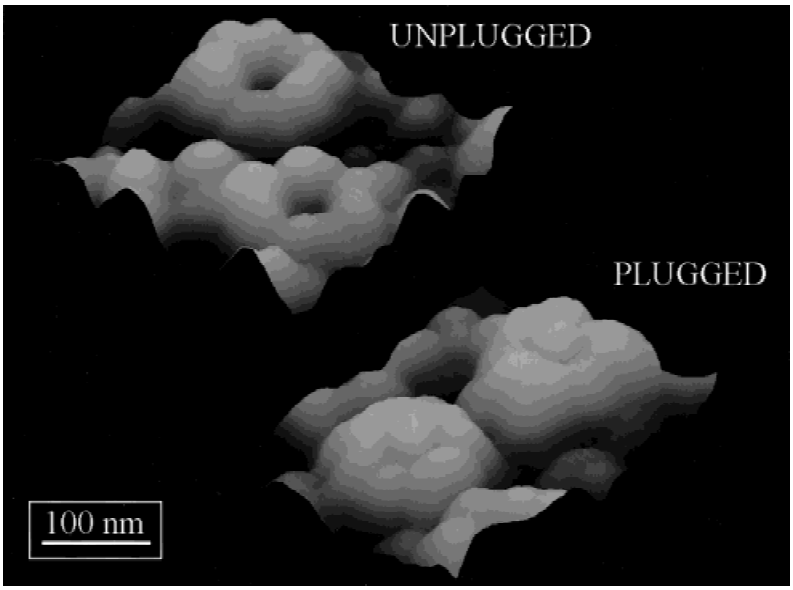

Fig. 2. Nuclear pore complexes in an air-dried nuclear envelope from *Xenopus laevis.* The upper left part of the figure shows two nuclear pores without visible central granules—''unplugged'' pores. The nuclear pores in the lower right part of the figure appear ''plugged'' with central granules.

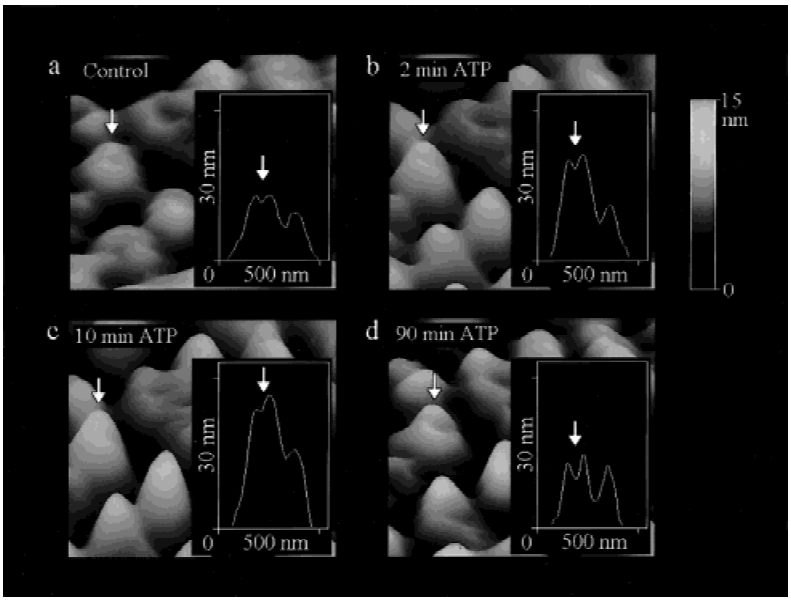

Fig. 3. (*a–d*). Individual patch of native nuclear pore complexes scanned in cytosolic electrolyte solution before (control) and during exposure to 1 mM ATP. (*a*) Control image obtained in the absence of ATP. (*b*) 2 min after exposure to ATP the nuclear pores grow in height and shrink in diameter. (*c*) 10 min after the addition of ATP nuclear pore ''contraction'' is most prominent. (*d*) 90 min after ATP exposure nuclear pores approach again control values (transient response to ATP). The insets in the figure show the change in profile of a single nuclear pore complex (marked in the respective AFM images and in the profiles by an arrow) over time.

tion, in another series of experiments we applied a slow-hydrolyzing ATP analogue to the isolated nuclear envelope preparation. Figure 5 shows two images obtained from the same local spot of the isolated nuclear envelope before (control) and 10 min after the addition of ATP-γ-S. As apparent from this figure, NPCs remain virtually unchanged. The central channels of the nuclear pores (unusually well visible in this particular preparation) remain relaxed (i.e., cytoplasmic orifices are open). Figure 6 shows a representative paired experiment, in which 10 NPCs were analyzed for changes in height and diameter. A summary of the ATP-γ-S experiments, performed on 10 nuclear envelopes is shown in Table 2. The same experimental protocol was used as described above for the ATP experiments. In none of the experiments nuclear pores exhibited any significant changes in height or diameter. The mean height and diameter values presented in Table 2 were measured in images recorded before (control) and 10 min after the addition of ATP-γ-S.

Discussion

Applying the AFM on nuclear envelopes in fluid, we were able to visualize the response of native nuclear

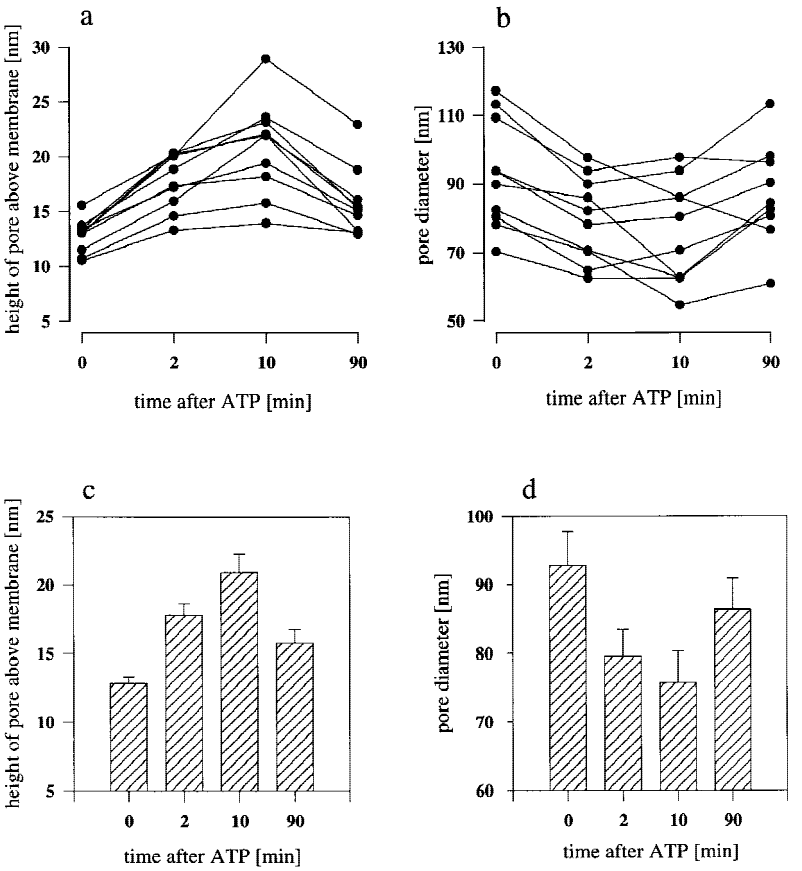

Fig. 4. (*a* and *b*). Individual heights of 10 nuclear pore complexes taken from the same nuclear envelope (measured from the cytoplasmic leaflet of the nuclear envelope to the top of the NPCs) and their diameters measured before (0 min ATP) and 2, 10 and 90 min after the addition of ATP. (*c* and *d*) Mean heights and diameters (±SEM) of the 10 nuclear pore complexes shown as individual data above (*a* and *b*). Nuclear pore heights and diameters show significant changes already two minutes after the addition of ATP ($P < 0.01$). This paired experiment was repeated several times in different nuclear envelopes with similar quantitative results (for further details *see* Materials and Methods).

Table 1. Shape of nuclear pore complexes (NPCs) before (control) and 10 min after addition of 1 mM ATP

Nuclear envelope	NPC height			NPC diameter		
	Control (nm)	ATP (nm)	Δ height (%)	Control (nm)	ATP (nm)	Δ diameter (%)
I	12.9 ± 0.62	22.0 ± 1.70	68.9 ± 9.44	91.8 ± 4.90	74.3 ± 4.82	−19.2 ± 2.80
II	14.1 ± 0.51	22.3 ± 1.29	58.1 ± 7.75	95.4 ± 4.90	77.5 ± 4.89	−18.9 ± 2.72
III	13.2 ± 0.63	22.4 ± 1.71	68.6 ± 8.97	94.3 ± 4.85	76.4 ± 4.87	−19.1 ± 2.85
IV	14.3 ± 0.60	23.3 ± 1.71	64.9 ± 9.03	95.1 ± 4.89	77.2 ± 4.89	−19.0 ± 2.73
V	11.6 ± 0.60	20.5 ± 1.68	77.5 ± 11.01	92.4 ± 4.90	74.4 ± 4.89	−19.6 ± 2.82
VI	14.0 ± 0.63	23.1 ± 1.63	64.1 ± 8.31	95.0 ± 4.89	77.1 ± 4.88	−19.0 ± 2.72
VII	12.7 ± 0.63	21.9 ± 1.70	71.3 ± 9.40	93.7 ± 4.89	75.8 ± 4.89	−19.2 ± 2.77
VIII*	11.6 ± 0.64	11.5 ± 0.71	−1.2 ± 1.50	92.9 ± 5.04	93.6 ± 5.14	0.8 ± 1.03
IX*	12.6 ± 0.66	12.7 ± 0.57	0.9 ± 1.78	94.5 ± 4.50	95.3 ± 4.00	1.1 ± 0.94
X*	11.9 ± 0.61	12.1 ± 0.80	1.6 ± 3.38	94.1 ± 5.00	94.4 ± 4.80	0.5 ± 0.78

In each nuclear envelope (I–X) height and diameter of 10 nuclear pores were evaluated ($n = 10$; ± SEM). ''NPC height'' indicates the height of the ringlike structure protruding from the cytoplasmic face of the nuclear envelope. It was measured from the lipid bilayer to the NPC top. ''NPC diameter'' was taken from the highest oppositely located points of the cytoplasmic ring in the cross-section of the respective NPC. The asterisk (*) indicates nuclear envelopes that did not respond to ATP. They are listed as numbers VIII–X. NPC height and NPC diameter changes were statistically significant ($P < 0.01$) in envelope I–VII and not significant in VIII–X.

pores to ATP under physiological conditions. The results of our paired experiments demonstrate a dramatic but transient change in NPC conformation following the addition of ATP. The nuclear pores increase strongly in height and decrease in diameter. To exclude possible artefacts caused by prolonged scanning and/or addition of fluid during the experiment we analyzed preparations scanned over 90 min adding the same amount of NIM

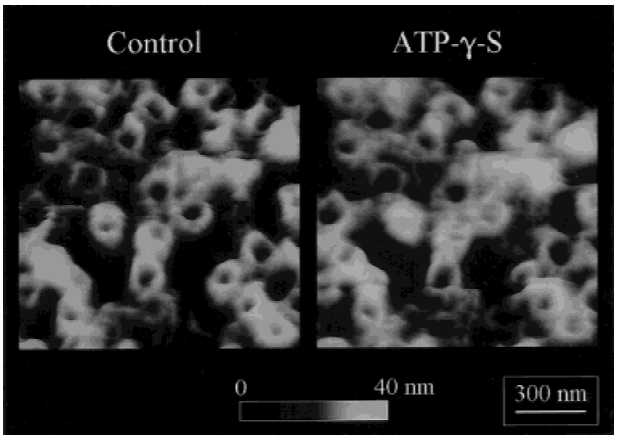

Fig. 5. AFM images obtained from the same patch of the isolated nuclear envelope of *Xenopus laevis* oocyte before (control) and 10 min after the addition of 1 mM ATP-γ-S. NPCs in this particular preparation have wide-open orifices protruding from the cytoplasmic face of the nuclear envelope.

without ATP. Our control experiments showed that addition of the mentioned volume did not introduce any artefacts (e.g., thermal shift). The NPCs in those preparations remained unchanged. To avoid any damage to the preparation scanning forces were constantly kept at minimal values. Furthermore, artefacts related to increased scanning forces would result rather in an apparent decrease but not in an increase of the nuclear pore height as observed in this study.

The observed ATP-induced NPC change may play a role as one of several important steps occurring during nucleocytoplasmic transport of macromolecules through the nuclear pore. The nature of a putative ATPase responsible for the observed conformational change is unknown. In 1986, Berrios and Fisher [4] discovered a myosin heavy chainlike ATPase associated with the nuclear envelope in higher eukaryotic cells. Using immunofluorescence and immunoelectron microscopy the same authors showed some years later that heavy chain like polypeptide, a nonmuscle isoform of myosin, is associated with the nuclear pore complex [5]. It has been previously proposed that a contractile apparatus may be involved in the nucleocytoplasmic transport of macromolecules through the NPC [17, 33]. A model was developed proposing that the nuclear pore contains eight myosin molecules arranged in an octagonal array with their heads facing the cytoplasm and their tails pointing toward the nucleus. These molecules are in contact with another eight myosin molecules arranged in opposite direction, with their heads facing the nucleoplasm. According to this model the bidirectional transport of macromolecules through the pore would be accomplished by a peristaltic wave of contractions generated by ATP hydrolysis in the myosin heads at the margins of the nuclear pore complex [4]. Other experimental findings also support the hypothesis of contractile elements playing a role in nucleocytoplasmic transport. Indeed, it has been reported that in addition to the myosin heavy chain, actin was also associated with the nuclear pore [3]. Furthermore, Schindler and Jiang [33] showed that the transport of certain dextrans through the NPCs was found enhanced by 250% after the addition of 3 mM ATP. The use of antibodies against actin or myosin inhibited the stimulating effect of ATP on the nucleocytoplasmic transport through NPCs.

The transient change in NPC shape monitored with AFM after the addition of ATP supports the transport model proposed by Berrios and Fisher [4]. The recorded shape change of the NPC, comparable to a contraction, observed on the cytoplasmic side of the nuclear envelope could represent the beginning of the proposed peristaltic wave activated through ATP hydrolysis by circularly arranged myosin heads or another (yet unknown) ATPase. The present experiments applying the slow-hydrolyzing ATP analogue, ATP-γ-S, to the nuclear envelope preparation clearly suggest that hydrolysis (and not binding) of ATP is necessary to induce the conformational change of the NPC. However, our studies only support but do not prove the model that nuclear pores ''contract'' in response to ATP.

The concentration of calcium ions is of crucial importance in actin-myosin interaction [36]. Recently the role of calcium in regulating nucleocytoplasmic transport has been elucidated. There is increasing evidence for the active involvement of calcium stored in intracellular compartments mediating transport through the NPC. The space between the two membranes of the nuclear envelope, the perinuclear cisternae, is continuous with the lumen of the endoplasmic reticulum, serving as a major intracellular calcium store [9, 26]. Greber and Gerace [14] reported that the depletion of calcium of the endoplasmic reticulum and the nuclear envelope using ionophores and calcium pump blockers, inhibited passive diffusion and active signal-mediated transport into the nucleus. Stehno-Bittel et al. [35] showed further evidence for the calcium dependence of nuclear transport when they inhibited the diffusion of intermediate-sized molecules into the nucleus, applying inositol 1,4,5-triphosphate ($Ins(1,4,5)P_3$) to release calcium from the stores or using calcium chelators to inactivate free calcium inside the nuclear stores. Thus, intracellular calcium store is most likely a prerequisite for normal function of nuclear pores. The mechanism by which a nuclear pore ''measures'' free calcium inside the nuclear envelope is yet unknown. However, a good candidate for a cisternal ''calcium sensor'' that could transfer the message (namely whether the calcium store is full or empty) to the nuclear pore could be a previously identified nuclear pore protein, gp210 [14]. This pore protein

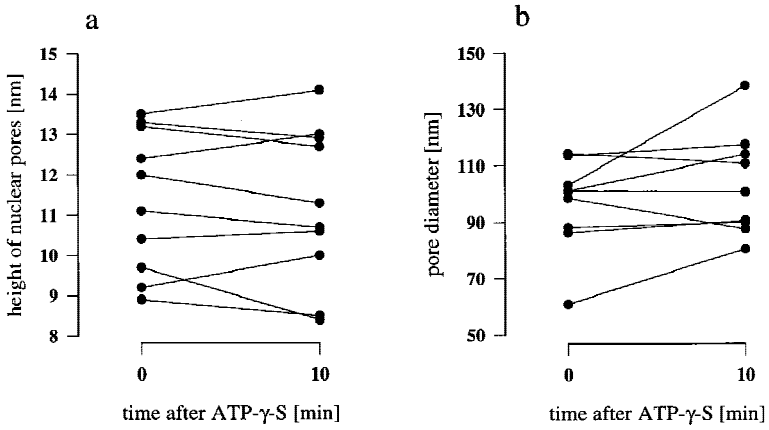

Fig. 6. Individual heights of 10 nuclear pore complexes (measured from the cytoplasmic leaflet of the nuclear envelope to the top of the pores) and their diameters measured before (0 min ATP) and 10 min after the addition of the slow-hydrolyzing ATP analogue, ATP-γ-S.

Table 2. Shape of nuclear pore complexes (NPCs) before (control) and 10 min after addition of 1 mM ATP-γ-S

Nuclear envelope	NPC height			NPC diameter		
	Control (nm)	ATP-γ-S (nm)	Δ height (%)	Control (nm)	ATP-γ-S (nm)	Δ diameter (%)
I	18.4 ± 1.99	17.7 ± 2.26	−5.5 ± 3.48	100.4 ± 3.99	104.0 ± 5.54	3.6 ± 3.81
II	11.4 ± 0.55	11.2 ± 0.61	−1.4 ± 2.03	97.0 ± 3.96	99.1 ± 3.42	2.5 ± 1.44
III	11.2 ± 0.50	10.9 ± 0.46	−1.8 ± 3.24	97.5 ± 4.83	99.4 ± 3.96	2.5 ± 2.15
IV	15.2 ± 0.73	14.8 ± 0.88	−2.5 ± 3.48	82.4 ± 7.90	81.2 ± 6.50	0.6 ± 4.21
V	13.8 ± 1.03	14.0 ± 0.85	2.0 ± 2.35	90.1 ± 5.02	91.1 ± 5.02	1.2 ± 1.37
VI	12.3 ± 0.64	12.2 ± 0.29	1.3 ± 4.41	96.3 ± 5.96	97.7 ± 5.67	1.6 ± 1.33
VII	12.1 ± 0.58	11.8 ± 0.48	−2.1 ± 3.30	95.5 ± 6.61	96.5 ± 5.73	1.7 ± 1.27
VIII	11.7 ± 0.55	11.6 ± 0.57	−0.2 ± 3.76	94.9 ± 4.20	96.8 ± 3.28	2.6 ± 1.97
IX	11.1 ± 0.55	10.9 ± 0.55	−1.6 ± 3.32	98.4 ± 3.84	98.4 ± 4.27	−0.2 ± 1.00
X	11.1 ± 0.48	11.1 ± 0.45	0.7 ± 1.77	98.7 ± 2.02	99.2 ± 1.62	0.6 ± 1.11

In each nuclear envelope (I–X) height and diameter of 10 nuclear pores were evaluated ($n = 10$; ± SEM). ''NPC height'' indicates the height of the ringlike structure protruding from the cytoplasmic face of the nuclear envelope. It was measured from the lipid bilayer of the nuclear envelope to the NPC top. ''NPC diameter'' was taken from the highest oppositely located points of the cytoplasmic ring in the cross-section of the respective NPC. NPC height and NPC diameter changes were statistically not significant in all nuclear envelopes.

contains multiple calcium binding domains, which are predicted to reside within the perinuclear space.

A filled cisternal calcium store could shift the nuclear pore into a transport mode that allows interaction of contractile elements within the NPC. Low levels of calcium inside the store, on the other hand, could reduce actin/myosin interaction leading to a change in the configuration of the NPC. Indeed, Perez-Terzic et al. [32] recently presented evidence for the existence of at least two distinct conformational states of the nuclear pore complex dependent upon cisternal calcium.

Recently, the role of GTP in nucleocytoplasmic transport has been intensively investigated [22]. The hydrolysis of GTP by Ran, a small nucleoplasmic and cytosolic GTPase belonging to the *ras* superfamily of proteins, was shown to provide at least a part of the energy required for the import of proteins. However, the involvement of other GTPases cannot be excluded. Experiments performed recently in our laboratory indicate that the exposure to 1 mM GTP (in the absence of Ran) does not trigger a visible change in nuclear pore shape. Upon addition of GTP the heights and diameters of NPCs remain virtually unchanged (unpublished data from our laboratory). This was not surprising, considering the absence of Ran. Nevertheless, it indicated an apparent lack of intrinsic GTPase activity within the nuclear pore complex (assuming that such a putative GTPase activity was associated with a NPC shape change).

Taken together, the nucleocytoplasmic translocation process presumably involves several conformational changes of the NPC that occur in a specific (not yet defined) time sequence. This indicates that the NPC structure is more dynamic than previously assumed.

We thank Drs. Michele Mazzanti (University of Milano, Italy) and Jose-Omar Bustamante (University of Sao Paulo, Brazil) for helpful discussions on nuclear pore structure and function during the course of the experiments. We gratefully acknowledge the continuous support

and interest in nuclear pores of our ''other'' membrane physiologists in the Physiological Institute of Würzburg and the valuable technical help of Birgit Gassner and Barbara Schuricht. The study was supported by the Deutsche Forschungsgemeinschaft, SFB 176 (A6) and OB 63-8.

References

1. Akey, C.W. 1995. Structural plasticity of the nuclear pore complex. *J. Mol. Biol.* **248:**273–93
2. Akey, C.W., Radermacher, M. 1993. Architecture of the *Xenopus* nuclear pore complex revealed by three-dimensional cryo-electron microscopy. *J. Cell Biol.* **122:**1–19
3. Bachs, O., Lanini, L., Serratosa, J., Coll, M.J., Bastos, R., Aligue, R., Rius, E., Carafoli, E. 1990. Calmodulin-binding proteins in the nuclei of quiescent and proliferatively activated rat liver cells. *J. Biol. Chem.* **265:**18595–600
4. Berrios, M., Fisher, P.A. 1986. A myosin heavy chain-like polypeptides is associated with the nuclear envelope in higher eukaryotic cells. *J. Cell Biol.* **103:**711–24
5. Berrios, M., Fisher, P.A., Matz, E.C. 1991. Localization of a myosin heavy chainlike polypeptide to Drosophila nuclear pore complexes. *Proc. Natl. Acad. Sci. USA* **88:**219–23
6. Bustamante, J.O., Liepins, A., Prendergast, R.A., Hanover, J.A., Oberleithner, H. 1995. Patch clamp and atomic force microscopy demonstrate TATA-binding protein (TBP) interactions with the nuclear pore. *J. Membrane Biol.* **146:**263–72
7. Feldherr, C.M., Kallenbach, E., Schultz, N. 1984. Movement of a karyophilic protein through the nuclear pores of oocytes. *J. Cell Biol.* **99:**2216–22
8. Folprecht, G., Schneider, S., Oberleithner, H. 1996. Aldosterone activates the nuclear pore transporter in cultured kidney cells imaged with atomic force microscopy. *Pfluegers Arch* **432:**831–8
9. Gerasimenko, O.V., Gerasimenko, J.V., Tepikin, A.V., Petersen, O.H. 1995. ATP-dependent accumulation and inositol triphosphate- or cyclic ADP-ribose-mediated release of Ca^{2+} from the nuclear envelope. *Cell* **80:**439–44
10. Goldberg, M.W., Allen, T.D. 1992. High resolution scanning electron microscopy of the nuclear envelope: demonstration of a new, regular, fibrous lattice attached to the baskets of nucleoplasmic face of the nuclear pores. *J. Cell Biol.* **119:**1429–40
11. Goldie, K.N., Pante, N., Engel, A., Aebi, U. 1994. Exploring native nuclear pore complex structure and conformation by scanning force microscopy in physiological buffers. *J. Vac. Sci. Technol.* **12:**1482–5
12. Görlich, D., Mattaj, I.W. 1996. Nucleoplasmic transport. *Science* **271:**1513–8
13. Görlich, D., Vogel, F., Mills, A.D., Hartmann, E., Laskey, R.A. 1995. Distinct functions for the two importin subunits in nuclear protein import. *Nature* **377:**246–8
14. Greber, U.F., Gerace, L. 1995. Depletion of calcium from the lumen of endoplasmic reticulum reversibly inhibits passive diffusion and signal-mediated transport into the nucleus. *J. Cell Biol.* **128:**5–14
15. Hinshaw, J.E., Carragher, B.O., Milligan, R.A. 1992. Architecture and design of the nuclear pore complex. *Cell* **69:**1133–41
16. Lal, R., John, S.A. 1994. Biological applications of atomic microscopy. *Am. J. Physiol.* C1–C21
17. LeStourgeon, W.M. 1978. The occurrence of contractile proteins in nuclei and their possible functions. *The Cell Nucleus* **VI.** 305–26
18. Loewenstein, W.R., Kanno, Y. 1962. Some electrical properties of the membrane of a cell nucleus. *Nature* **195:**462–4
19. Matzke, A.J.M., Weiger, T.M., Matzke, M.A. 1990. Detection of a large cation-selective channel in nuclear envelopes of avian erythrocytes. *FEBS Lett.* **271:**161–4
20. Mazzanti, M., Innocenti, B., Rigatelli, M. 1994. ATP-dependent ionic permeability on nuclear envelope in in situ nuclei of *Xenopus* oocytes. *FASEB J.* **8:**231–6
21. Moore, M.S., Blobel, G. 1992. The two steps of nuclear import, targeting to the nuclear envelope and translocation through the nuclear pore, require different cytosolic factors. *Cell* **69:**939–50
22. Moore, M.S., Blobel, G. 1994. A G protein involved in nucleocytoplasmic transport: the role of ran. *TIBS* **19:**211–6
23. Moroianu, J., Blobel, G., Radu, A. 1995. Previously identified protein of uncertain function if karyopherin alpha and together with karyopherin beta docks import substrate at nuclear pore complexes. *Proc. Natl. Acad. Sci. USA* **92:**2008–11
24. Newmeyer, D.D., Finlay, D.R., Forbes, D.J. 1986. In vitro transport of a fluorescent nuclear protein and exclusion of non-nuclear proteins. *J. Cell Biol.* **103:**2091–102
25. Newmeyer, D.D., Forbes, D.J. 1988. Nuclear import can be separated into distinct steps in vitro: nuclear pore binding and translocation. *Cell* **52:**641–53
26. Nicotera, P., McConkey, D.J., Jones, D.P., Orrenius, S. 1989. ATP stimulates Ca^{2+} uptake and increases the free Ca^{2+} concentration in isolated rat liver nuclei. *Proc. Natl. Acad. Sci. USA* **86:**453–7
27. Nigg, E.A. 1997. Nucleocytoplasmic transport: signals, mechanisms and regulation. *Nature* **386:**779–87
28. Oberleithner, H., Brinckmann, E., Schwab, A., Krohne, G. 1994. Imaging nuclear pores of aldosterone sensitive kidney cells by atomic force microscopy. *Proc. Natl. Acad. Sci. USA* **91:**9784–8
29. Paine, P.L., Moore, L.C., Horowitz, S.B. 1975. Nuclear envelope permeability. *Nature* **254:**109–14
30. Pante, N., Aebi, U. 1993. The nuclear pore complex. *J. Cell Biol.* **122:**977–84
31. Pante, N., Aebi, U. 1994. Towards understanding the three-dimensional structure of the nuclear pore complex at the molecular level. *Curr. Opin. Struct. Biol.* **4:**187–96
32. Perez-Terzic, C., Pyle, J., Jaconi, M., Stehno-Bittel, L., Clapham, D.E. 1996. Conformational states of the nuclear pore complex induced by depletion of nuclear calcium stores. *Science* **273:** 1875–7
33. Schindler, M., Jiang, L.-W. 1986. Nuclear actin and myosin as control elements in nucleocytoplasmic transport. *J. Cell Biol.* **102:**859–62
34. Schneider, S., Folprecht, G., Krohne, G., Oberleithner, H. 1995. Immunolocalization of lamins and nuclear pore complex proteins by atomic force microscopy. *Pfluegers Arch* **430:**795–801
35. Stehno-Bittel, L., Perez-Terzic, C., Clapham, D.E. 1995. Diffusion across the nuclear envelope inhibited by depletion of the nuclear Ca^{2+} store. *Science* **270:**1835–8
36. Szent-Gyorgyi, A.G. 1975. Calcium regulation of muscle contraction. *Biophys. J.* **15:**707–23